american physiological society

JNP JOURNAL OF NEUROPHYSIOLOGY

J Neurophysiol 135: 51–64, 2026.
First published December 1, 2025; doi:10.1152/jn.00458.2025

RESEARCH ARTICLE

Higher Neural Functions and Behavior

From low-level to high-level factors' influence on pupil hippus

Vivien Rabadan,* Maria Rosa Bufo,* Camille Ricou, Nadia Aguillon-Hernandez, Yassine Mofid, and Claire Wardak

Université de Tours, INSERM, Imaging Brain & Neuropsychiatry iBraiN U1253, Tours, France

Abstract

Pupil diameter, controlled by the autonomic nervous system (ANS), reflects numerous processes, from arousal to cognitive functions. In particular, the characteristics of the pupil at rest, its size and dynamics, reflect the tonic activity of the ANS. However, which factor can influence these pupillary characteristics at rest remains unclear. The pupil exhibits a physiological rhythmic oscillation, called hippus, which remains poorly characterized. Our aim was to better characterize the hippus by investigating how its parameters were influenced by different low- (illumination) and high-level (executive functioning) conditions. Pupil size variations of 30 adults (19–35 yr old) were recorded during five randomly appearing blocks. Although always requiring central fixation, the blocks varied according to gradients of illumination (11-lx, 19-lx, and 28-lx) and cognitive load (fixation, dot counting, and mental subtraction). Three main parameters were assessed: the median pupil diameter, the frequency, and amplitude of the hippus. Increasing illumination yielded smaller pupils and reduced hippus amplitude, while hippus frequency remained stable. In contrast, distinct effects were observed for the two high-level conditions. High cognitive load produced sustained pupil dilation and heightened hippus frequency, while intermediate counting showed minimal change except a decrease in hippus amplitude. Individual baseline pupil size was predictive of the amplitude of changes induced by the parameters. Our findings suggest that resting-state pupil oscillations are modulated differentially by low- and high-level influences, likely via integrative structures such as the locus coeruleus and superior colliculus, but also by biomechanical constraints.

NEW & NOTEWORTHY We demonstrate, for the first time in a single within-subject protocol, how low-level (illumination) and high-level (cognitive load) factors differentially shape both baseline pupil size and the oscillatory hippus. Bright light drives tonic constriction and reduces hippus amplitude probably via iris biomechanics, while mental effort elicits dilation and increases hippus frequency through central arousal circuits. Individual resting-pupil profiles predict the amplitude of these responses.

autonomic nervous system; cognitive; eye-tracking; illumination; oscillation

INTRODUCTION

Since the past century, the variation of pupil size has been systematically observed in clinical examinations and in research. Pupil size variation is a key element (1) that reflects the autonomic nervous system activity (ANS) (2) and depends on the contractile activity of the iris. The pupil diameter is governed by two antagonist muscles: the dilator of the iris under sympathetic control and the pupillae sphincter under parasympathetic control (for a recent review, see Ref. 3). When there is a change in the illumination condition, the pupillary light reflex induces a pupillary constriction via the parasympathetic pathway (4, 5). When the illumination is stable, pupil dilation, controlled through the sympathetic pathway, can be observed in several sensory or cognitive contexts (4). Dilation and constriction, thus, are studied as indicators of the functioning of the sympathetic and parasympathetic autonomic nervous system, respectively (6). However, these two phenomena are transitory, and the two systems interact to enable a dynamic balance of the pupil diameter. Pupil diameter is influenced by many factors that can induce constriction, such as environmental lighting (7), or dilation, such as cognitive engagement (8). These two types of factors can be considered as low-level and high-level factors, referring to the processing of light and focal distance, and executive functions, respectively (9).

*V. Rabadan and M. R. Bufo contributed equally to this work.
Correspondence: C. Wardak (claire.wardak@univ-tours.fr).
Submitted 12 September 2025 / Revised 18 October 2025 / Accepted 24 November 2025

Pupil diameter has been extensively studied as an index of arousal states and their fluctuations (3) and exhibits a particular dynamic for low levels of arousal. Indeed, at rest, pupil fluctuations, known as hippus, have been observed but are not well defined in the current literature yet. The term hippus has been used for many centuries and was already used by Hippocrates and Galen (10). Though it has been frequently associated with pathology, like epilepsy (11, 12), it is a physiological and ubiquitous phenomenon (10, 13) occurring in adults and children (14). Yoss et al. (13) define hippus as follows: "an inconstant spontaneous bilateral synchronous rhythmic constriction and [dilation] of the pupils of sufficiently large amplitude to be easily visible to the clinician."

The origin of this oscillatory behavior is still unclear, and some studies have tried to correlate hippus frequency with various physiological signals [like BOLD (blood-oxygen-level dependent) signal, heart rate variability, or respiration (15–17)]. Turnbull et al. (18), by locally (at the eye level) and selectively inhibiting either the parasympathetic (with tropicamide) or the sympathetic (phenylephrine) branch of the ANS, suggest that hippus is modulated only by the parasympathetic nervous system (18, 19). However, there is also increasing evidence that hippus may be controlled by the rivalry of sympathetic and parasympathetic activation (11, 12, 14). In fact, Centeno et al. (11) and Fernández-Torre et al. (12) suggest hippus could be due to cyclic periods of sympathetic activation followed by a rebalancing or increase of parasympathetic tone (postictal phase). Moreover, Bufo et al. (14) find a correlation between the hippus frequency and peaks of electrodermal activity that tends to support this hypothesis. Furthermore, Schaefer et al. (17) showed that slow pupil oscillations can partially phase-lock with respiration, consistent with an autonomic contribution. However, this coupling appears state dependent and may be attenuated under higher cognitive engagement (20). Its strength also varies across individuals and experimental paradigms (21).

As an oscillation, hippus can be described by two main parameters: the frequency and amplitude of the cycles. Several studies attempted to calculate the frequency of this hippus. Hippus frequency is frequently reported below 0.3 Hz (14, 16, 22, 23), but without real consensus, questioning sometimes the similitude of the recorded signals or the methodology of analysis. Indeed, the different recording parameters and the processing steps that allow to obtain this principal frequency are rarely described, which does not allow real reproducibility of the measurements. Studies of the pupil at rest have mainly focused on the median pupil diameter and have rarely described or estimated hippus frequency and amplitude.

Median pupil diameter is modulated by numerous factors. Two main low-level factors have been studied: illumination, with a larger constriction for high illumination (5, 24), and wavelength, with a larger dilation for increasing wavelengths (25). For high-level factors, an increase in cognitive or mental load and/or difficulty of the task induces a larger pupil dilation (26). It has been proposed that the size of the pupil, through its modulation by the locus coeruleus, is an indicator of the level of activity of the central nervous system (27, 28).

The amplitude of the hippus is also modulated by low-level and high-level factors. Parnandi et al. (16) have shown that hippus is present for different illumination levels. In addition, low ambient light induces greater hippus amplitude (16, 29). However, hippus frequency does not seem to be affected by illumination (16). So far, studies have shown that the hippus disappears when a mental activity such as arithmetic is carried out (11, 22). It is unclear yet if hippus characteristics depend on a unique regulatory process or are the result of interacting factors.

Despite the work carried out previously, few studies have properly assessed both hippus frequency and amplitude, and their relationship with the pupil size. Moreover, the respective influence of illumination and mental load conditions has never been directly compared. To tackle these issues, we examine the impact of low-level (illumination) and high-level (cognitive load) factors on pupil variation. Within the framework described by Strauch et al. (9), an intermediate level of engagement (i.e., pupil response related to attention orientation) was, however, constant throughout the experiment thanks to a fixation task.

We used a resting fixation protocol with different light levels to assess the effect of low-level factors processing, and two cognitive tasks to assess the effect of high-level factors modulation. Although both pupil median and hippus seem controlled by the balance between parasympathetic and sympathetic inputs, no studies have yet tried to assess the relationship between these measures. Based on the literature, the covariation of these measures seems to diverge between low-level and high-level contexts. Indeed, for the effect of illumination levels, we could expect a larger median pupil size and a larger hippus amplitude for low illumination (15, 16, 18, 29, 30), but without any change in frequency (15, 16, 18). For different mental loads, we could expect the median pupil diameter to increase (26) and the hippus to decrease in amplitude or even disappear (22) with increasing mental load. Evaluating these parameters in the same individuals, in contexts varying for low-level and high-level factors, would help shed light on the mechanisms influencing pupil parameters.

METHODS

Participants

Thirty adults (15 females) aged 19 to 43 yr old (means ± SD: 26.52 ± 5.99 yr) were included in this study. Noninclusion criteria were abnormal or uncorrected vision, history of psychiatric, neurological, or neurodevelopmental disorders and learning disabilities or difficulties, as well as the use of medications acting on the autonomic nervous system. Written informed consent was obtained from each adult before the experiment. The study was approved by an ethics committee (CPP, protocol PROSCEA 2017-A00756-47) and conformed with the Declaration of Helsinki ethical principles for medical research involving human subjects. No participant dropped out or was excluded from the analyses.

Stimuli and Protocol

As described in Fig. 1, five different blocks were created to assess the influence of the factors being studied. For clarity

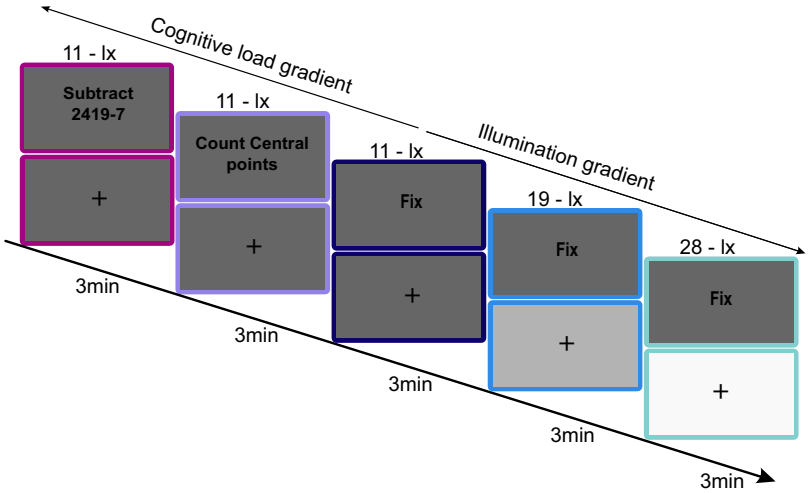

Figure 1. Protocol. Each block lasted 180 s and was preceded by a 4 s screen instructing the participant of the block that would be displayed. The five blocks were randomly presented during the recording. Colored contours code the nature of the block, as used in Fig. 3 and were not presented. The color code was as follows: subtract (magenta), count (purple), fixation (navy blue), 19-lx (light blue), and 28-lx (cyan).

in this manuscript, the term block will be used interchangeably with experimental condition. The protocol was designed around a fixation block of 11-lx of illumination. Two gradients emanated from this block: a first gradient of illumination going from the 11-lx to a 28-lx block via a 19-lx block (11-lx < 19-lx < 28-lx), and a second gradient of cognitive load [under constant illumination (11-lx)] going from the fixation block to the subtraction block via a counting block (fixation < count < subtract) (Fig. 1). The five blocks (i.e., experimental conditions) were presented once in a random order. The illumination gradient values were chosen to remain within the mesopic range of vision (10–30 lx), to optimize the balanced activity of cones and rods (31). The lower illumination block was set to 11 lx to avoid floor values, and an interval of 8–9 lx between blocks was chosen to provide sufficiently distinct illumination steps to elicit measurable differences in pupillary dynamics without inducing visual discomfort.

Illumination gradient.

For the three low-level blocks, i.e., the blocks along the illumination gradient, the participant only had to fixate a central cross. Each block lasted 180 s and began with a 4 s screen instructing the participant to fixate ("Fix"). The black fixation cross (width 1.80°, height 1.96°, and thickness 0.16°) was presented on a uniform gray background (11, 19, or 28-lx).

Cognitive load gradient.

For the blocks along the cognitive load gradient, the participant had to fixate a central cross presented on a uniform gray background (11-lx).

For the intermediate-level cognitive load block, i.e., the counting block, participants had to fixate the central cross and to mentally count the number of times they saw a white dot in the center of the cross. The standard fixation cross was presented but every 10 to 30 s, a white dot appeared at its center for 50 ms. This dot appeared 11 times, with the block lasting between 120.55 s and 360.55 s. The block started with a 4 s screen instructing the participant to "count central points." Participants had to verbally report the total number of counted dots at the end of the block.

For the high-level cognitive load block, i.e., the subtraction block, participants had to fixate the central cross and perform mental subtractions during the whole block. The block lasted 180 s and began with a 4 s screen instructing the participant to "subtract 2419 − 7." Then, only the standard fixation cross was presented on a uniform gray background (11-lx). Participants had to mentally perform successive subtractions until the end of the block (2419 − 7, then 2412 − 7, then 2405 − 7, etc.) and then report the result of their last subtraction at the end of the block. This result was not analyzed per se, as some subjects reportedly lost their count or made mistakes, but helped to ensure that the task was performed all along the block as instructed.

The tasks were explained to the participants before the start of the experiment. Participants were also asked to look at the screen and remain silent for the duration of the recording, except when reporting their answers.

Materials

Eye-tracking data were recorded by an SMI RED500 eye-tracker system (SensoMotoric Instruments GmbH, Germany), which was placed 2 cm below the screen. This eye tracker has a sampling rate of 500 Hz, a gaze position accuracy of 0.40°, and a tracking resolution of 0.03° of visual angle, and an optimal operating distance between 60 and 80 cm. It has a tracking range (headbox) of 40 × 20 cm and can support a head speed of up to 50 cm/s, with a gaze tracking range of 40° horizontally and 60° vertically. As reported by SMI, this tool takes into account slight head movements that have no effect on the calibration and resulting measurements. An influence of stimulus brightness and illumination on calibration is also reported. However, we performed the calibration on a 19-lx screen (using white points on a gray background), and the stimuli in our experiment ranged from 11 to 28 lx, with a maximum variation of 9 lx, which is considered a low variation in illumination.

Gaze and pupil data were recorded using iViewX 2.8. The protocol was run using Experiment Center 3.6. All recordings took place in the same experimental room with an ambient light level of 8 lx. In addition, all participants were comfortably seated in a chair in front of the screen (22 in. Dell P2213

monitor with a resolution of 1,680 × 1,050 px and a refresh rate of 59 Hz) at ~70 cm (measured by the eye tracker with a built-in laser meter software), separated from the experimenter by a curtain.

Before starting the eye-tracking recordings, a five-point calibration procedure was performed, followed by a four-point validation. Calibration was considered as correct if the precision calculated during the validation was below 1.00°. Otherwise, the calibration procedure was repeated until this precision was reached.

The room was illuminated by two 6 V DAYVIA adaptable LED lights positioned 5 cm either side of the screen. Illumination levels were measured with a Testo 545-lx meter with 1-lx resolution, placed at the eye level of the subject 70 cm away from the recording screen.

Data Processing

Raw signal processing.

The raw pupil data were exported from BegazeTM 3.6 software. Data processing was then performed using in-house MATLAB scripts [MATLAB v. 9.4.0.813654 (R2018a), Natick, MA; RRID:SCR_001622]. All processing steps are illustrated in Supplemental Fig. S1, and a summary of the processing is shown in Fig. 2.

First, the datasets were extracted according to the five experimental conditions. For each participant, we plotted the pupil diameter values to ensure data integrity. This step allowed us to verify that no anomalies were affecting the recordings (Supplemental Fig. S1*A* and Fig. 2*A*).

Next, we corrected blinks, which could interfere with the pupil diameter measurements. To do this, we first calculated the blink velocity derivative. This derivative enabled us to identify the start and end times of each blink. Once the blinks were identified, they were removed from the recordings for each eye. To compensate for the missing data, we interpolated the 70 pupil diameter values that preceded and followed each blink, ensuring data continuity.

After this correction, we averaged the pupil diameters for both eyes for each participant (Supplemental Fig. S1*B*).

Subsequently, to ensure the quality of the data, the recordings were trimmed by removing 10,000 points (20 s) at the beginning and end of each block. This step was intended to eliminate pupil variations caused by block transitions or instructions given to the participants, which could interfere with the measurements.

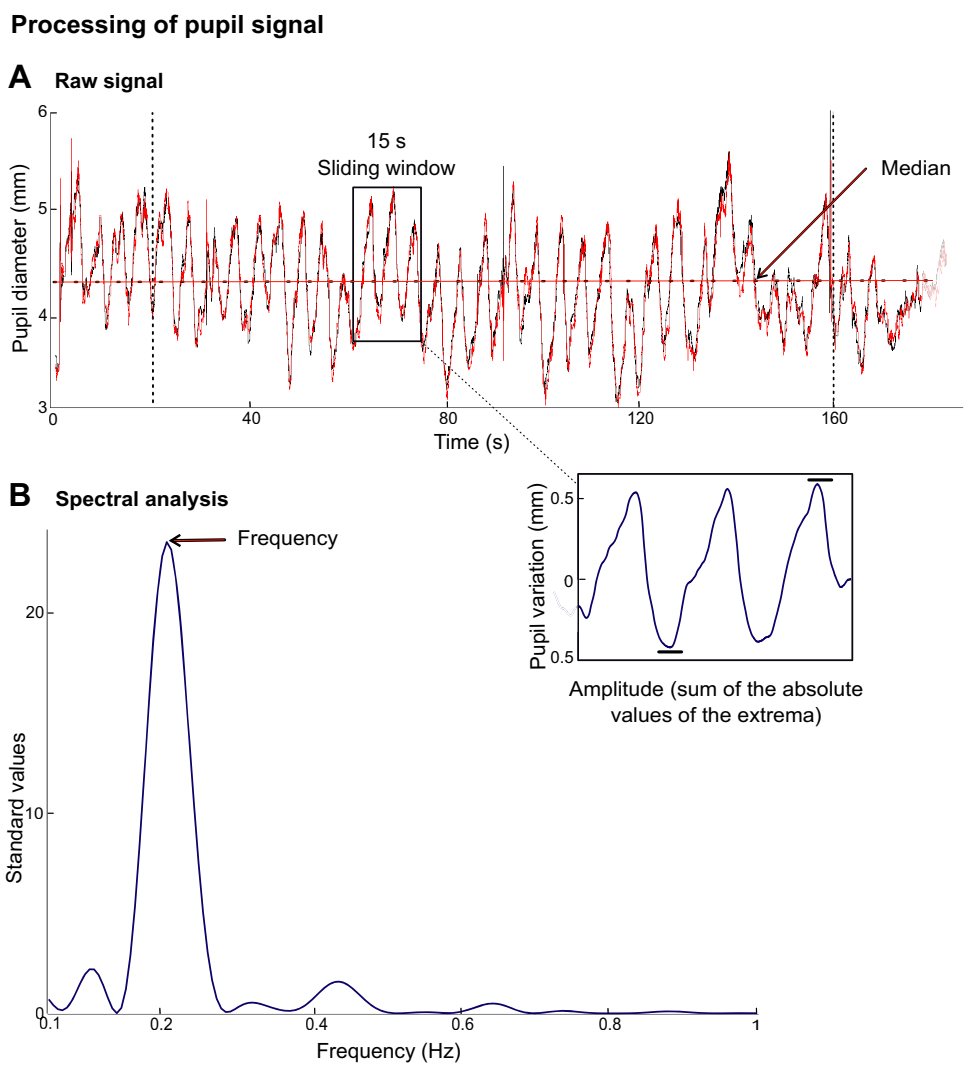

Figure 2. Signal processing of pupil recording data. *A*: raw signal. *Top*: continuous pupil diameter trace before interpolation and filtering. *Bottom, right*: 15-s zoom of the filtered trace illustrating individual hippus cycles and how oscillation amplitude is measured. *B*: spectral analysis. Power spectral density of the processed signal, showing the frequency bands of the hippus. Representative data from one participant.

Finally, for each block and participant, we calculated three parameters: the median pupil diameter, which represents the central value of the pupil diameter during each measurement period; the frequencies of pupil variation, which indicate the oscillations of the pupil diameter throughout the experiment; and the amplitude of these variations. The same procedure was applied for all blocks and all participants, with no blinding necessary considering the protocol.

Parameter extractions.

To assess pupil variations and their stability during each block, we performed a series of steps using a 15-s sliding window (with 1-s sliding steps, i.e., 93.33% overlapping) (Supplemental Fig. S1*C*). First, to obtain a spectrum of the signal, we applied *a*) a 1×3 one-dimensional median filter to smooth the signal and remove impulse noises, *b*) a second-order Butterworth bandpass filter with bandpass frequencies between 0.1 Hz and 1.0 Hz to remove the harmonic frequencies (Supplemental Fig. S1*D*), and *c*) a Fast Fourier Transform for spectral analysis (Supplemental Fig. S1*E* and Fig. 2*B*).

To carry out the spectral analysis over our 15-s sliding window while maintaining good resolution, we interpolated our 15-s signals using an 81,920-point nfft (nonuniform Fast Fourier Transform). Accuracy was therefore increased from 0.07 Hz to 0.0031 Hz [$\Delta f = (sf/(N*T)$; f: frequency in Hz, N: number of points = 81,920, sf: sampling frequency = 500 Hz, T: time in s = 15 s].

Once the frequency spectra were obtained, the maxima on each spectrum were labeled and extracted. Then, we calculated the median frequency and interquartile range over all the sliding windows.

When measuring amplitude, we applied a bandpass filter with bandpass frequencies of 0.1 Hz and 0.5 Hz to retain only the amplitude data from our signal that was relevant to the extracted frequencies. Then, still on the sliding window of 15 s, we measured the amplitude by adding up the absolute values of the extrema of a window. This gave us ~125 amplitude values for one block of stimuli for each participant.

Following these processing steps, we calculated the median frequency and interquartile range over all the sliding windows.

Additional processing.

Once the median, frequency, and amplitude parameters were extracted, they were organized into a file and normalized to facilitate data classification. Normalization was carried out based on the type of parameter, using a robust method: we subtracted the median of the entire dataset from the median of each parameter, then divided the result by the interquartile range of the dataset. This normalization enabled us to perform a clustering of the data.

We were also interested in the variability of the raw pupil signal, as well as in the dispersion of eye movements and blinks (see Supplemental Methods and Results).

Statistical Analyses

Statistical analyses were performed using RStudio [v4.1.1 (32)] on the following parameters: median pupil diameter, median frequency, interquartile frequency, median amplitude, and interquartile amplitude. The influence of illumination (3 conditions: 11-lx, 19-lx, and 28-lx) and cognitive load (3 conditions: fixation, dot counting, and subtraction) on the various parameters was evaluated using separate repeated-measures ANOVA, corrected by Greenhouse-Geisser, and supplemented with post hoc Bonferroni-adjusted multiple comparisons. We also examined, using a linear mixed model, whether age or sex influenced the studied parameters. *P* corrected values and effect sizes (η^2) are provided for each effect. For all parameters, normality of distribution and homogeneity of variance were tested using the Kolmogorov–Smirnov and Levene tests.

Verification of the assumptions of normality and homogeneity of the data.

Before proceeding with our statistical tests, we ensured that the assumptions of data normality and homogeneity of variances were met. Normality was assessed using the Kolmogorov–Smirnov (KS) test via the *stats* package (33) in R. Homogeneity of variances was checked using the levene_test () function from the *car* package (34), which tests for equality of variances across groups. Furthermore, to detect the presence of outliers in our data series, we calculated the lower and upper limits using the following formula: lower limit = Q1 − 1.5 × IQR and upper limit = Q3 + 1.5 × IQR (IQR: interquartile range, Q1 and Q3: first and third quartiles, respectively).

ANOVA and post hoc test.

For repeated-measures ANOVA, we used the aov () function from the *stats* package (33). Once the ANOVA was performed, we applied the pairwise.t.test () to compare all pairs of groups. The *P* values were adjusted using the Bonferroni method to account for multiple comparisons. In our analyses, three comparisons were conducted for each condition.

Data analysis with LMM.

The linear mixed model (LMM) was used to analyze the relationships between an independent variable (sex and age) and several dependent variables (our parameters). In the R software, we fitted the model using the lmer () function from the lme4 package (35), and to test the fixed effects and obtain the relevant statistical parameters, we used the Anova () function from car package (34).

Normalization and clustering.

For data normalization, we applied the median () and IQR () functions to perform robust normalization. This approach is less sensitive to outliers and contributes to improved stability in the analyses. The clustering was run on a participant-by-feature matrix with one row per participant ($n = 30$) and 15 columns corresponding to the median of three pupillary parameters (pupil diameter, hippus frequency, and hippus amplitude) computed in each of the five experimental conditions (Fix-11 lx, Fix-19 lx, Fix-28 lx, Count-11 lx, and Subtract-11 lx). Only medians were used as features for clustering; IQRs were not included. Next, for clustering, we used the *cluster* (36) (RRID:SCR_013505) and *ggplot2* (37) (RRID: SCR_014601) packages to calculate silhouette scores and create elbow plots, which allowed us to determine an optimal

number of clusters (set to 2 in our study). The kmeans () function from the *cluster* package (36) was then used to perform unsupervised clustering. To visualize the results, we used *ggplot2* (37) to create the k-means related plots. Once clustering was performed, we extracted the centroids associated with the parameters of each group. To assess the performance of the classification model, we conducted a receiver operating characteristic (ROC) analysis. This analysis, carried out with custom MATLAB scripts, allowed us to calculate the AUC-ROC (area under the ROC curve) for each parameter, to compare the two groups and identify the most discriminative parameters. A model was considered to perform well if the AUC-ROC was greater than 0.8.

Correlations and data visualization.

To assess the monotonic relationships between the variables in our dataset, we used the Spearman correlation test. Significant correlations were considered when the absolute value of Spearman's correlation coefficient (rho) was greater than 0.5, and the P value was less than 0.05. The correlations were adjusted using the Bonferroni-correction method. We calculated the correlation matrix using the cor () function and used the *corrplot* package (38) to visualize this matrix graphically.

For the creation of the figures intended for the article, we used R software and the *ggplot2* package (37). Specifically, we used the geom_violin (), ggline (), and ggcorrplot () functions to create violin plots, line plots, and correlation matrix, respectively. These plots allow for a clear visual representation of the analysis results. To finalize the formatting of the figures, we used Inkscape software (v.0.92.3) (RRID:SCR_014479), which enables us to adjust graphical elements and enhance the presentation.

RESULTS

Pupillary Reactivity to Low-Level Processing

We analyzed how the median of the pupillary diameter, the frequency of the hippus (and its IQR), and hippus amplitude (and its IQR), varied depending on the illumination of the stimuli. We also controlled the effect of illumination on gaze dispersion as well as on the number and frequency of eye blinks (see Supplemental Results). In addition the effect of age and sex on these parameters was controlled.

We obtained a main effect of illumination [$F(2,58) = 61.416$; $P < 0.001$, $\eta 2 = 0.679$] on the median pupil diameter. Post hoc comparisons showed that higher illumination always led to a significantly smaller median pupil diameter (28-lx: 3.74 ± 0.5 mm, 19-lx: 4.02 ± 0.7 mm, 11-lx: 5.37 ± 0.9 mm; $P < 0.001$ for both comparisons 28-lx vs. 11-lx and 19-lx vs. 11-lx, $P < 0.01$ for 28-lx vs. 19-lx) (Fig. 3*A.1*).

There was also an effect of illumination on the hippus frequency. Although the median of the hippus frequency did not change [28-lx: 0.21 ± 0.02 Hz, 19-lx: 0.21 ± 0.03 Hz, 11-lx: 0.20 ± 0.03 Hz; $F(2,58) = 0.248$; $P > 0.05$, $\eta 2 = 0.008$], the interquartile range was significantly influenced by illumination [28-lx: 0.09 Hz, 19-lx: 0.07 Hz, 11-lx: 0.08 Hz; $F(2,58) = 4.102$; $P < 0.05$, $\eta 2 = 0.124$]. Post hoc comparisons showed a significantly higher interquartile range for the 28-lx condition compared with the 19-lx condition ($P < 0.05$) (Fig. 3*A.2*).

The amplitude of the hippus was impacted by the illumination. Indeed, we observed a main effect on the median amplitude of the hippus [28-lx: 0.34 ± 0.10 mm, 19-lx: 0.38 ± 0.13 mm, 11-lx: 0.40 ± 0.14 mm; $F(2,58) = 6.074$; $P < 0.01$, $\eta 2 = 0.173$], but not on the interquartile range [28-lx: 0.14 mm, 19-lx: 0.15 mm, 11-lx: 0.18 mm; $F(2,58) = 2.622$; $P > 0.05$, $\eta 2 = 0.083$]. Post hoc comparisons revealed that higher illumination led to a decrease in the amplitude of the hippus (28-lx vs. 11-lx, $P < 0.01$;) (Fig. 3*A.3*).

An assessment of the effects of sex and age showed there was no effect of sex on the parameters studied under the different illumination conditions. However, there was a main effect of age on the median pupil diameter [$F(1,28) = 7.305$; $P < 0.01$, $\eta 2 = 0.210$] and on the median [$F(1,28) = 12.156$; $P < 0.01$, $\eta 2 = 0.303$] and interquartile amplitude [$F(1,28) = 7.446$; $P < 0.05$, $\eta 2 = 0.210$] of the hippus. In fact, the younger the subject, the larger the median pupil diameter, the median amplitude, and the interquartile amplitude of the hippus.

We evaluated the link between pupil median, hippus frequency, and hippus amplitude within each condition by performing correlation analyses. We found a significant correlation only in the 28-lx condition, between the median pupil diameter and the amplitude of the hippus ($R = 0.503$, $P = 0.005$). As the pupil constricted, the amplitude of the hippus oscillation decreased (Supplemental Fig. S2).

We also analyzed the effect of low-level illumination on gaze and blinks (see Supplemental Fig. S3), and observed only an effect of illumination on vertical gaze position, without any significant correlation with our pupil median or hippus parameters.

Pupillary Reactivity to High-Level Processing

For the effect of cognitive load, we analyzed how the median pupil diameter, the hippus frequency (and its IQR), and amplitude (and its IQR) varied as a function of the workload of the tasks for the three blocks with identical illumination. We also controlled the effect of cognitive load on gaze dispersion as well as on the number and frequency of eye blinks (see Supplemental Results). In addition, the effect of age and sex on these parameters was controlled.

There was a main effect of cognitive load [fixation: 5.37 ± 0.93 mm, count: 5.37 ± 0.91 mm, subtract: 6.64 ± 0.77 mm; $F(2,58) = 31,651$, $P < 0.001$, $\eta 2 = 0.522$] on the median pupil diameter. Post hoc comparisons confirmed that the median pupil diameter was significantly larger in the subtraction condition compared with the two other conditions, the count and fixation ($P < 0.001$ for both comparisons) (Fig. 3*B.1*).

We also found a significant effect of workload on the hippus frequency. Indeed, the interquartile range [fixation: 0.08 mm, count: 0.07 mm, subtract: 0.09 mm; $F(2,58) = 5.088$, $P < 0.05$, $\eta 2 = 0.149$] and the median [fixation: 0.20 ± 0.03 mm, count: 0.19 ± 0.02 mm, subtract: 0.23 ± 0.04 mm; $F(2,58) = 15.666$, $P < 0.001$, $\eta 2 = 0.351$] of hippus frequency showed a variation as a function of the condition. Post hoc comparisons revealed that the median of the hippus frequency was higher in the subtract condition than in the count condition ($P < 0.001$). Moreover, the interquartile range was significantly lower for the count

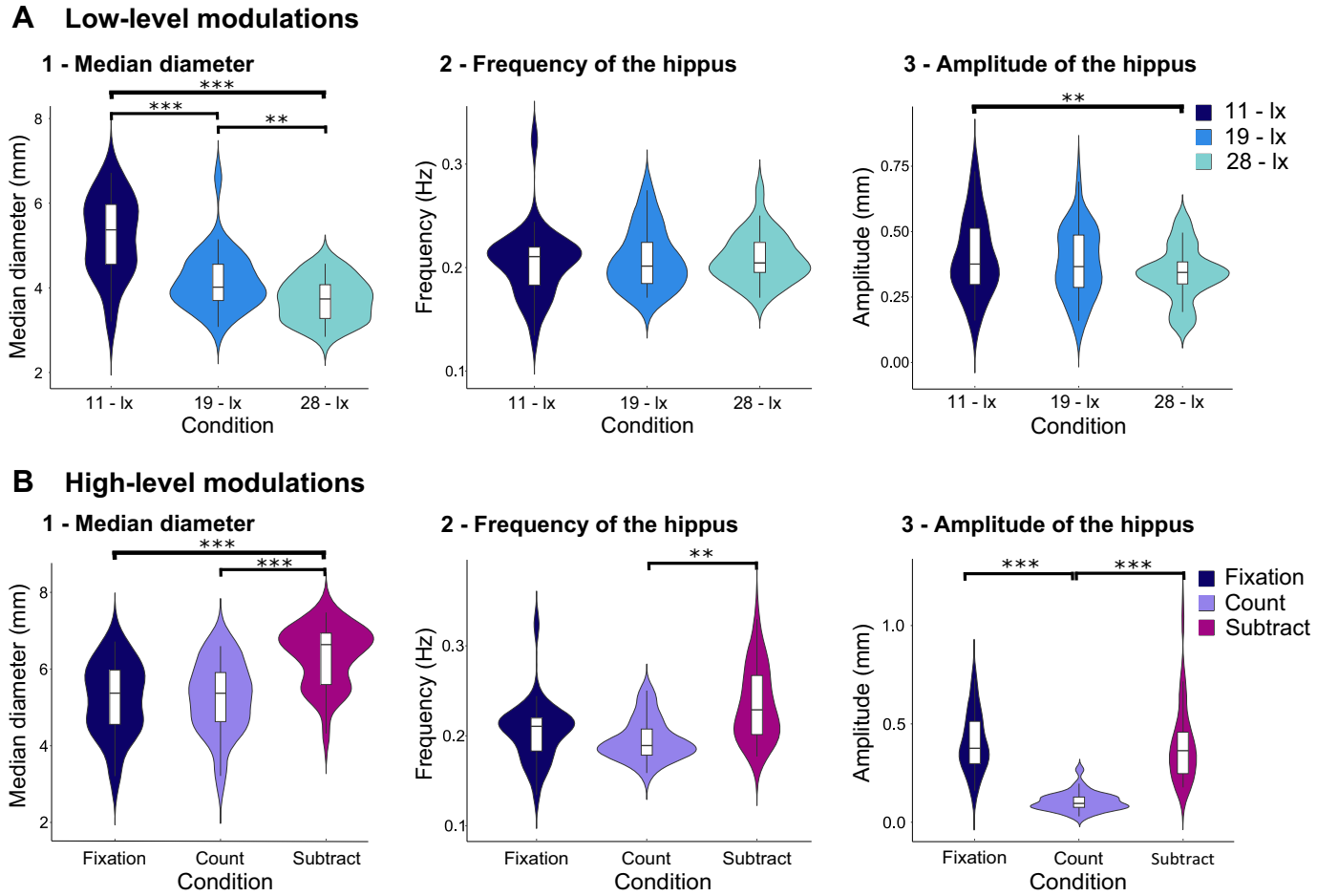

Figure 3. Low-level and high-level modulations on the median pupil diameter and on the pupil hippus under different conditions. *A*: low-level modulations on median diameter of the pupil (*A.1*, in mm), frequency of the hippus (*A.2*, in Hz), and amplitude of the hippus (*A.3*, in mm) for three luminosity conditions (11-lx in dark blue, 19-lx in medium blue, 28-lx in light blue). *B*: high-level modulations on median diameter of the pupil (*B.1*, in mm), frequency of the hippus (*B.2*, in Hz), and amplitude of the hippus (*B.3*, in mm) for three cognitive load conditions (fixation in dark blue, count in purple, subtract in magenta). $n = 30$ participants, repeated mesures ANOVA with post hoc comparisons: $^{***}P < 0.001$, $^{**}P < 0.01$.

condition compared with the two other conditions (subtract and fixation) ($P < 0.05$ for both comparisons) (Fig. 3*B.2*).

An effect on the amplitude of the hippus was also observed. Indeed, the interquartile range [fixation: 0.18 mm, count: 0.08 mm, subtract: 0.18 mm; $F(2,58) = 14.185$; $P < 0.001$, $\eta 2 = 0.328$] and the median [fixation: 0.40 ± 0.14 mm, count: 0.11 ± 0.04 mm, subtract: 0.39 ± 0.19 mm; $F(2,58) = 58.174$; $P < 0.001$, $\eta 2 = 0.667$] showed an effect of the condition on the amplitude. The post hoc comparisons confirmed that both parameters were lower in the count condition compared with the two other conditions, subtract and fixation ($P < 0.001$ for both comparisons) (Fig. 3*B.3*).

An assessment of the effects of sex and age showed that there was no effect of sex on the parameters studied under the different workload conditions. However, there was a main effect of age on the median pupil diameter [$F(1,28) = 10.509$; $P < 0.01$, $\eta 2 = 0.273$] and on the median [$F(1,28) = 10.351$; $P < 0.01$, $\eta 2 = 0.270$] and interquartile amplitude [$F(1,28) = 8.992$; $P < 0.01$, $\eta 2 = 0.243$] of the hippus. In fact, the younger the subject, the larger the median pupil diameter, the median amplitude, and the interquartile amplitude of the hippus.

We evaluated the link between pupil median, hippus frequency, and hippus amplitude with each block by performing correlation analyses and found no significant correlations.

We also analyzed the effect of high-level factors on gaze and blinks (see Supplemental Fig. S3) and observed small effects on vertical gaze position and blink frequency, without any significant correlation with our pupil median or hippus parameters.

Pupillary Reactivity across Luminosity and Cognitive Conditions

To explore the relationship between variations observed along both the low-level and high-level gradients, we used two complementary approaches: a clustering approach and a correlation approach.

First, we conducted a clustering analysis on individual data, which allowed us to identify two distinct clusters: a "large pupil" cluster, consisting of 12 participants, and a "small pupil" cluster, consisting of 18 participants. Both these clusters were affected by the experimental conditions. Regarding the median and frequency parameters, individuals in the "large pupil" cluster consistently exhibited higher median and frequency values, regardless of the condition type, with a parallel evolution to that of the "small pupil"

cluster, but a larger increase in hippus frequency in the Subtract condition (Fig. 4, *A* and *B*). In contrast, for the amplitude parameter, no similar pattern was observed (Fig. 4*C*). Both clusters evolved similarly, with no qualitative distinction between the groups, regardless of the recording condition.

To evaluate this classification, we used the ROC method, which allowed us to validate the quality of a binary classification. We set an AUC-ROC threshold of 0.8 to consider a parameter as a good classifier. This allowed us to highlight four parameters that effectively distinguished the "large pupil" and "small pupil" clusters. The area under the curve (AUC) for the pupil median in the cognitive conditions (Fixation 11-lx: 0.8148, Count: 0.8055, Subtract: 0.8009), as well as for the frequency of hippus in the Subtract condition (0.9653), showed strong discriminative power. The "large pupil" cluster exhibited larger pupil median and a higher hippus frequency (Fig. 4, *A* and *B*).

Second, to correlate variations of pupil parameters across the low-level and high-level gradients, for each individual and parameter, we used the parameters values in the Fixation 11-lx condition as a reference (this reference corresponds to the "Baseline" in Fig. 5). We thus computed the variation between any given condition with this reference and performed correlation analyses between reference values (Fix-11-lx) and the absolute variation for all parameters (delta high cognitive level for Subtract vs. Fix-11-lx; delta low cognitive level for Count vs. Fix-11-lx; delta high illumination level for Fix-28-lx vs. Fix-11-lx; delta low illumination level for Fix-19-lx vs. Fix-11-lx).

For the median pupil diameter, we observed a high correlation between the value in the reference condition (Fix-11-lx) and the delta of the high cognitive level ($R = 0.68$, $P = 5.047 \times 10^{-5}$), the delta of the low illumination level ($R = 0.82$, $P = 9.507 \times 10^{-7}$), as well as the delta of high illumination levels ($R = 0.85$, $P = 7.091 \times 10^{-7}$). Consequently, we also observed significant correlations between these three deltas (delta high cognitive vs. delta low illumination: $R = 0.75$, $P = 5.049 \times 10^{-6}$; delta high cognitive vs. delta high illumination: $R = 0.71$, $P = 2.225 \times 10^{-5}$; delta high illumination vs. delta low illumination: $R = 0.94$, $P = 2.17 \times 10^{-8}$). In other terms, and going beyond what was observed at the cluster levels, the larger the median pupil diameter in the reference condition (Fix-11-lx), the larger the effect of the Subtract condition. Participants with larger pupils in a resting fixation condition showed larger cognitive engagement indexed by median pupil diameter. Moreover, those individuals with larger pupil at rest were also the most influenced by changes in illumination. Another smaller but significant correlation was observed between the delta of low cognitive level and the delta of low illumination level ($R = 0.55$, $P = 0.0018$) (Fig. 5*A*).

For the hippus frequency, this analysis revealed an effect not observed when comparing conditions at the group level, nor by the cluster analysis. Indeed, we observed significant correlations along the illumination gradient, between the value in the reference condition (Fix-11-lx) and the delta of the high illumination level ($R = 0.69$, $P = 2.324 \times 10^{-5}$), as well as between the delta of low and high illumination ($R = 0.52$, $P = 0.003$). The larger the hippus frequency in the reference condition, the larger the variation induced by changes in illumination, i.e., the lower the frequency at high illumination level (Fig. 5*B*).

For the amplitude of the hippus, the correlation analysis reinforced the results observed at the group level. Indeed, at the group level, we observed a significant difference in hippus amplitude between our reference condition (Fix-11-lx) and both the high illumination condition (Fix-28-lx) and the low cognitive condition (Count). The correlation analysis revealed that, for the individuals with the higher hippus amplitude in the reference condition, a larger variation was observed for both the other conditions (correlation between

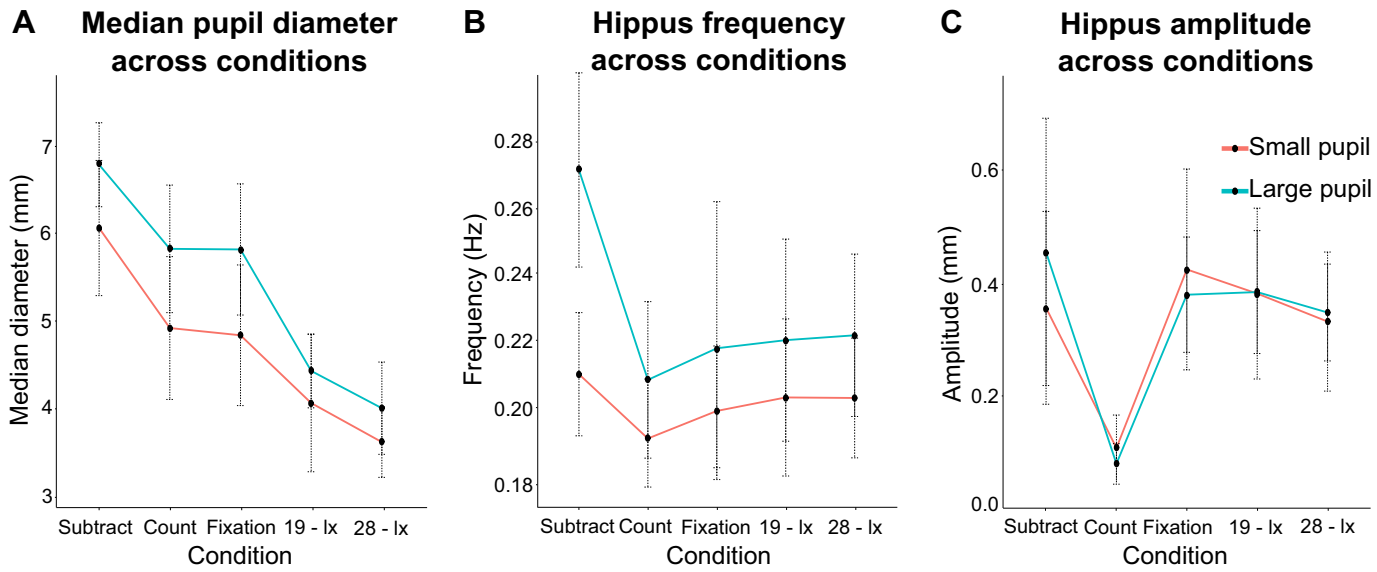

Figure 4. Distinct pupillary profiles revealed by clustering. *A*: median pupil diameter across conditions for "small-pupil" (red) and "large-pupil" (green) clusters; lines connect condition means intracluster. *B*: hippus frequency across the same conditions and clusters. *C*: hippus amplitude across the same conditions and clusters. In all panels, conditions are ordered left to right as follows: subtract, count, fixation, 19 - lx, 28 - lx. Error bars represent the 95% confidence interval around each cluster mean. $n = 30$ participants, k-means clustering.

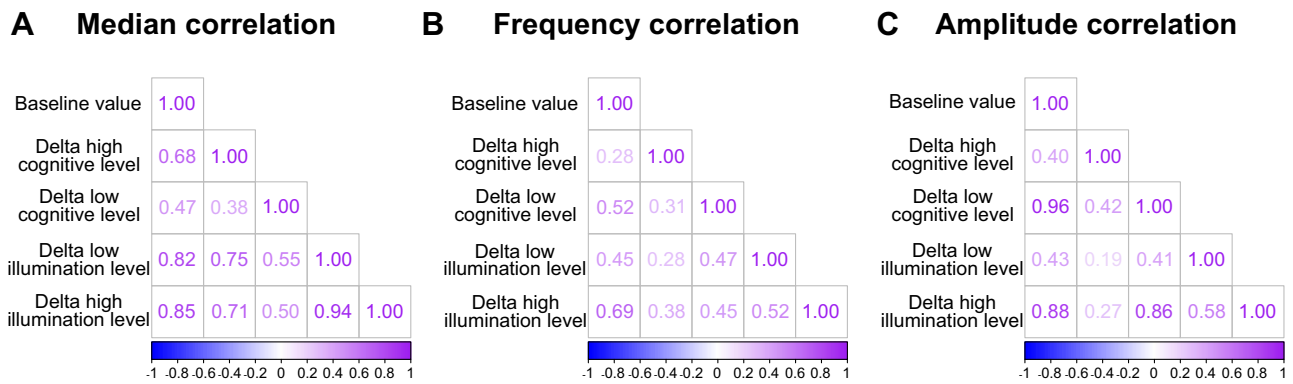

Figure 5. Correlation matrices of baseline and condition-induced changes. *A*: median pupil diameter correlations. *B*: hippus frequency correlations. *C*: hippus amplitude correlations. In each panel, Spearman's rank ρ is computed between the baseline value (Baseline corresponds to the Fixation 11-lx condition) and the change observed under four conditions: high cognitive load, low cognitive load, low illumination, and high illumination. Correlation coefficients are color-filled on a blue-purple gradient: dark blue for strong negative and dark purple for strong positive correlations. Numerical ρ values are shown in each cell. $n = 30$ participants.

reference value and delta low cognitive level: $R = 0.96$, $P = 2.2 \times 10^{-16}$; correlation between reference value and delta high illumination level: $R = 0.88$, $P = 4.587 \times 10^{-7}$). Consequently, these variations were also correlated with each other (delta low cognitive level and delta high illumination: $R = 0.86$, $P = 6.42 \times 10^{-7}$). Finally, along, the illumination gradient, we also observed a significant correlation between the deltas of low and high illumination levels ($R = 0.58$, $P = 0.001$) (Fig. 5*C*).

To go further and estimate possible correlations across parameters, we used the same approach but on normalized data, with a unique analysis factoring all the deltas. No significant interparameter correlations emerged; however, the same intraparameter relationships were replicated.

DISCUSSION

In this study, we used eye-tracking to investigate the pupil and its dynamics in response to variations in high-level and low-level factors during a head-free fixation task in adults. To our knowledge, the effects of high- and low-level processing on the pupil and its hippus have never been studied within a single protocol in the same individuals. In our study, we observed a significant impact of illumination and cognitive load on the pupil and its dynamics.

We observed that increasing ambient illumination produced a progressive and significant reduction in median pupil diameter accompanied by a decrease in hippus amplitude, while overall hippus frequency remained unchanged but its interquartile range increased under the brightest condition. Cognitive load likewise modulated pupillary behavior. During the mental subtraction task, median pupil diameter increased by over 1 mm compared with fixation and counting, and hippus frequency and variability were elevated. Although the intermediate counting task elicited a marked reduction in hippus amplitude. Gaze dispersion showed a vertical but not horizontal sensitivity to illumination, with minimal effects of cognitive load, and blink rate and number remained largely invariant across all conditions, ruling out oculomotor artifacts. Cluster analysis revealed two distinct participant profiles ("large pupil" vs. "small pupil") distinguished primarily by median diameter and hippus frequency, and correlation analyses demonstrated that baseline pupil metrics strongly predicted both illumination and cognition-induced changes. This pattern of results highlights both common and dissociable mechanisms by which low- and high-level factors shape pupillary dynamics.

Tonic Light-Driven Constriction with Unchanged Hippus Rhythm

Prolonged exposure to increasing light levels produced the anticipated sustained constriction of pupil diameter, with median values falling from 5.37 mm in dark gray (11-lx) to 3.74 mm under bright illumination (28-lx). This tonic adaptation is driven by the classical parasympathetic pupil light reflex pathway: glutamatergic signals from rods and cones, together with slower melanopsin-mediated input from ipRGCs (intrinsically photosensitive retinal ganglion cell), converge on the pretectal olivary nucleus (PON), which transmits them via the central mesencephalic reticular formation to the Edinger–Westphal nucleus (EW), from which parasympathetic fibers travel through the ciliary ganglion to activate the iris sphincter (4, 39). Concomitantly, hippus amplitude diminished as luminance increased, suggesting elevated reflexive tone preventing iris activity (16, 18, 40). In contrast, hippus frequency remained stable across light levels, suggesting that its pacing originates from a distinct central oscillator rather than peripheral mechanics.

Mechanical Restraint of Hippus Amplitude at High Luminance

Under the brightest illumination (28-lx), we observed both a pronounced reduction in hippus amplitude and a significant broadening of its frequency distribution. These dual effects stem from sustained, strong contraction of the iris sphincter, which increases iris rigidity beyond the critical pupil size thresholds [~3.36mm for constriction and 5.72mm for dilation; Loewenfeld (41)] and thus mechanically limits oscillation amplitude. At the same time, fluctuations in central arousal likely contribute to the broader spread of hippus frequencies. Indeed, Reimer et al. (28) linked slow oscillations in pupil size to variations in autonomic tone, and more

recent work has shown that tonic firing of locus coeruleus neurons correlates with increased variability in pupil-oscillation timing (42). Crucially, only at 28 lx did median diameter and hippus amplitude correlate. Participants whose pupils constricted more under bright light showed the greatest reduction in oscillation size. This relationship underscores that, under high luminance, peripheral iris mechanics, rather than central timing mechanisms, limit oscillatory amplitude.

Even as descending inputs from the frontal eye fields (FEF) and lateral intraparietal area (LIP) pass through the intermediate layers of the superior colliculus (SCi) to modulate pupillary tone (43–46), ipRGC-driven and noradrenergic influences continue to generate rhythmic drive (42). Under these conditions, the sphincter muscle remains in sustained, strong contraction. As a result, the stiffened iris cannot deform sufficiently to translate these central signals into large-amplitude hippus. Consequently, high-luminosity conditions reveal a clear dissociation: central arousal mechanisms persist in altering frequency, but mechanical constraints of the iris impose a hard limit on amplitude.

Modulation of Pupil by Cognitive Load

Beyond the purely light-driven control of pupil size, evidence implicates central neuromodulatory and oculomotor circuits in adjusting pupil diameter according to cognitive and attentional demands. Phasic increases in locus coeruleus (LC) firing, driven by salient or effortful mental events, produce transient dilations (42, 47). Tonic LC activity, in turn, sets baseline pupil diameter in line with arousal and sustained attention (48, 49).

Simultaneously, preparatory activity in frontal eye fields (FEF) and lateral intraparietal area (LIP) can bias local pupil size in anticipation of forthcoming foveal targets (44, 50). Together, these pathways enable the pupil to reflect both mental load (e.g., working memory, calculation) and visuospatial attention, effectively tuning retinal input to task demands.

Enforced fixation dampens hippus.

In the count task, where cognitive demand is moderate, the anticipated tonic pupil dilation did not occur. Rather, hippus amplitude fell, and its variability was suppressed, even though the median diameter remained unchanged. This flat pupillary profile under mental load mirrors previous observations, in which the system prioritizes energetic economy over sensory gain (51, 52). Besides, the need for strict oculomotor fixation on the central cross likely drives sustained activation of the sphincter, increasing iris solicitation, and suppressing microsaccade-related pupillary perturbations. Hafed and Krauzlis (53) showed that enforced fixation suppresses microsaccades and reduces associated transient pupil fluctuations, while Loewenfeld (41) demonstrated that continuous sphincter contraction attenuates spontaneous hippus amplitude. Furthermore, our correlation analysis revealed a strong relationship between the reduction in hippus amplitude between fixation to counting and that between fixation to high luminance ($R = 0.86$, $P = 6.42 \times 10^{-7}$). This cross-condition association shows that parasympathetic sphincter activation constrains hippus amplitude in both tasks, albeit through distinct mechanisms: enforced fixation during counting continually solicits the iris sphincter (53) while sustained, high-tension contraction under bright illumination pushes the iris beyond its critical size thresholds, mechanically limiting oscillation amplitude (41).

High load boosts pupillary rhythm.

By contrast, the high-load subtraction task elicited both a robust median dilation of over 1mm and a significant increase in hippus frequency, effects that align with both tonic and phasic activation of the locus coeruleus-noradrenergic system (52, 54). Sustained cognitive effort engages tonic LC activity to raise baseline pupil size (48, 49), while real-time performance monitoring triggers phasic noradrenergic bursts that manifest as more frequent oscillations (42, 55). Krejtz etal. (56) further demonstrated that these higher-frequency oscillations closely track moment-to-moment attentional fluctuations, suggesting that the elevated hippus in the subtraction condition reflects transient shifts in vigilance. Notably, subtraction increased hippus frequency without reducing amplitude, indicating that even under intense cognitive strain, the iris sphincter retains sufficient contractile flexibility to convey central arousal via oscillation rate (55, 57, 58).

The two tasks thus show a clear dissociation: counting produced reduced hippus amplitude with little change in frequency, whereas subtraction drove both elevated baseline diameter and heightened oscillatory frequency. This pattern highlights a dual regulation of hippus: peripheral oculomotor control acting on the sphincter sets amplitude limits (53, 59), while central attentional circuits, especially via the locus coeruleus, govern oscillation frequency (28, 42, 46). Preparatory signals from the FEF and LIP can adjust the tonic and phasic modes of the LC, thereby modulating the timing of pupillary responses (3, 60).

Layered Regulation of Pupil Dynamics

Our correlation analyses show that individual baseline pupil metrics predict both illumination- and cognition-induced changes, indicating a shared susceptibility of the pupillary system to central and peripheral drives (Fig. 6). Median pupil diameter, as outlined above, reflects parasympathetic gain via the pupil light reflex pathway (4) and is further modulated by tonic locus coeruleus activity under cognitive load (48, 49), as well as by preparatory signals conveyed via the SCi from FEF and LIP (3, 44, 50). Hippus amplitude likewise reflects parasympathetic tone but is constrained by the mechanical properties of the iris. Once sphincter contraction increases iris rigidity beyond a critical threshold, further changes in tone translate poorly into oscillation size (41). By contrast, hippus frequency appears governed by purely central mechanisms. It remains stable across light levels yet rises under high cognitive demand via phasic locus coeruleus bursts (42, 55) and may be paced by oculomotor rhythms mediated through SCi projections (46). Together, these findings reveal a triple dissociation in pupillary control (Fig. 6): *1*) median diameter reflects an interplay of parasympathetic gain and attentional anticipation;

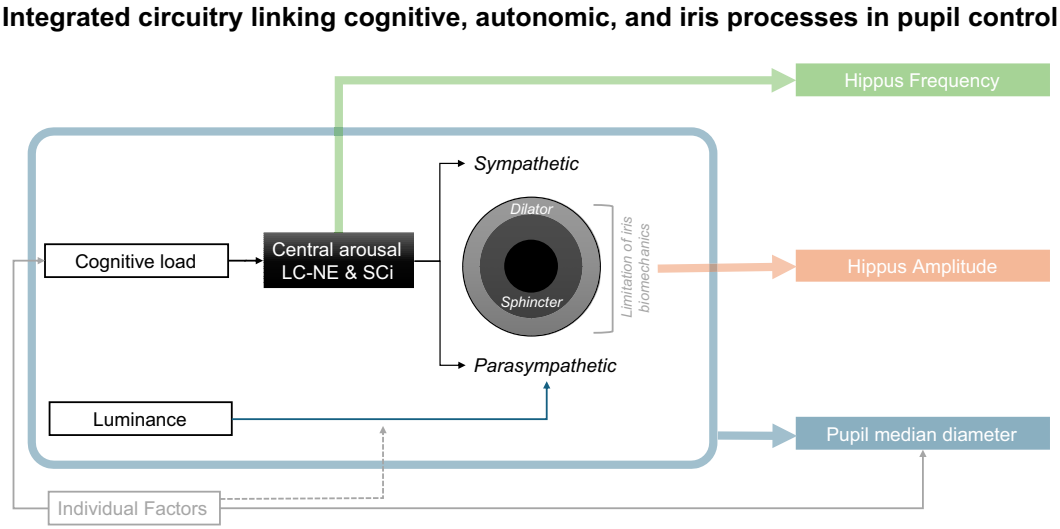

Figure 6. Integrated circuitry linking cognitive, autonomic, and iris processes in pupil control. This schematic illustrates how luminance and cognitive load inputs lead to different pupillary outcomes. The outputs are color-coded: median pupil diameter (blue), hippus frequency (green), and hippus amplitude (orange). Arrows indicate the direction of influence across the cognitive, autonomic, and iris levels. In addition, the influence of individual factors is shown in gray.

2) amplitude is constrained by iris biomechanics; while *3*) frequency indexes central arousal pacing. This layered regulation enables the pupil to integrate low-level sensory inputs and high-level cognitive states.

Impact of the Pupil Profile

Our cluster analysis revealed two stable participant profiles, "large pupil" and "small pupil," across both illumination and cognitive conditions. Individuals in the "large pupil" cluster exhibited higher median diameters and hippus frequencies regardless of task or light level, whereas those in the "small pupil" cluster showed consistently smaller values. This finding mirrors prior work showing that baseline pupil size indexes differences in arousal system sensitivity and behavioral performance. Larger resting pupils correlate with elevated tonic locus coeruleus activity and superior sustained-attention performance (49, 61), while smaller resting pupils are linked to greater internal attention or mind-wandering tendencies (62). Crucially, our correlation analyses demonstrated that baseline metrics recorded during simple fixation at 11 lx strongly predicted subsequent changes under bright illumination and high cognitive load. This suggests a common autonomic set point governing pupillary reactivity. Previous research indicates that individuals with larger resting pupils not only exhibit greater constriction in response to increased luminance (4, 49) but also display more pronounced dilations under cognitive load, reflecting elevated tonic locus coeruleus activity (48). Similar baseline-dependent effects have been observed in human EEG pupil couplings, where larger pupils predict greater task-evoked dilations (63), and in rodent LC-pupil dynamics (55). Our data suggest that a larger resting pupil permits a greater proportional constriction, while smaller baseline pupils allow for larger proportional dilations. In other words, when starting from a larger baseline, the iris can constrict by a higher fraction of its diameter, whereas a smaller starting diameter affords more room for relative dilation. This distinction highlights that baseline size not only determines iris reactivity but also shapes the dynamic range of autonomic responses (49, 64). The dissociation between amplitude and frequency control further underscores individual differences. "Large pupil" individuals showed both greater amplitude modulation under light and steeper increases in frequency with cognitive load. In contrast, small-pupil participants exhibited blunted responses in both domains. This pattern aligns with models proposing that baseline arousal state gates both peripheral contractility and central noradrenergic responsiveness (47). Practically, baseline pupil clustering may serve as a noninvasive predictor of an individual's susceptibility to attentional lapses or sensory overload, with potential applications in clinical assessment of disorders marked by dysregulated arousal.

Limitations and Perspectives

Although our data clearly demonstrate that pupil diameter reflects integrated sensory and cognitive modulations, several limitations warrant emphasis. First, luminance was intentionally held constant during the cognitive tasks to isolate load-related effects and to keep sessions brief, thereby preserving participants' attention, so our design does not directly test the full interaction between illumination and cognitive load within a single unified task. Future studies should therefore implement a fully crossed within-task manipulation with multiple luminance levels and parametric cognitive load (65). Second, the link between neuronal activity and pupil dilation remains indirect: the correlation between LC activity and pupil diameter varies significantly from neuron to neuron (42), indicating that pupillometry reflects the sum of multiple central influences (PON, SCi, LC, cortex) modulated by the experimental context. Third, slow oscillations in pupil diameter remain challenging to interpret. The literature describes a broad frequency range (0.03–0.3 Hz) depending on paradigms: Loewenfeld (41) reported hippus centered around 0.05 Hz at rest, Yellin et al. (66)

observed fluctuations at 0.03–0.1 Hz correlated with cortical transitions in fMRI, and Reimer et al. (28) highlighted a 0.1–0.2 Hz band related to vigilance states in rodents. In our protocol, the median frequency of 0.2 Hz lies at the upper end of these distributions, likely due to prolonged visual constraint, focus on the fixation cross, and absence of complete rest phases between blocks, favoring faster autonomic components. Because we lack a consensus on what each frequency band represents, there is a clear need in the literature to characterize these various oscillations, both why their peak frequencies differ across studies and precisely what each band represents in terms of neural or autonomic origins. In addition, respiration may contribute to slow pupillary oscillations via autonomic pathways. Because respiration was not recorded here, future work should incorporate concurrent respiratory monitoring to test for breathing-hippus coupling and quantify how it varies with cognitive engagement. Consequently, these observations call for multimodal approaches: combining EEG to better characterize cortical rhythms, fMRI to localize sources, and pharmacological protocols targeting adrenergic and cholinergic pathways will allow dissection of the respective contributions of the SCi, LC, and prefrontal cortex to each frequency band. Such studies are essential for pupil diameter tracking to become a robust biomarker of attentional and arousal states.

In summary, our findings demonstrate that pupil dynamics emerge from the interplay of parasympathetic gain, iris biomechanics, and central arousal circuits (Fig. 6). Individual resting pupil size provides a crucial baseline that predicts both light- and task-evoked responses. Hippus oscillations, whose amplitude is constrained by iris physiology and whose frequency reflects locus coeruleus-mediated arousal, provide a noninvasive index of brain state. Future studies combining pupillometry with neuroimaging and pharmacological manipulations will be essential to disentangle these mechanisms and to validate both baseline pupil metrics and hippus characteristics.

DATA AVAILABILITY

Source data for this study are not publicly available due to privacy or ethical restrictions. The source data are available to verified researchers upon request by contacting the corresponding author.

SUPPLEMENTAL MATERIAL

Supplemental Material, Results, and Figs. S1–S3: https://osf.io/xhfwk/overview?view_only=b45777cafded4f3e9ed3885330c9001f.

ACKNOWLEDGMENTS

Present address of M. R. Bufo: Aix Marseille University, CRPN (Centre de recherche en psychologie et neuroscience – UMR 7077), CNRS, Marseille, France.

GRANTS

PhD fellowship for V.R. is funded by the Fondation de France (Allocation jeunes chercheurs en ophtalmologie et neuro-ophtalmologie 2022) and the FEANS (Fondation Européenne pour l'Avancement des Neurosciences). PhD fellowship for M.R.B. was funded by the FEANS. PhD fellowship for C.R. was funded by the ANR (ANR-21-CE17-0045-01). The project is funded by FHU-Exac-t (EXcellence Center for Autism – Tours).

DISCLOSURES

No conflicts of interest, financial or otherwise, are declared by the authors.

AUTHOR CONTRIBUTIONS

C.W. conceived and designed research; V.R., M.R.B., C.R., and C.W. performed experiments; V.R., M.R.B., and Y.M. analyzed data; V.R., N.A-H., and C.W. interpreted results of experiments; V.R. prepared figures; V.R. and C.W. drafted manuscript; V.R., M.R.B., N.A-H., Y.M., and C.W. edited and revised manuscript; V.R., M.R.B., C.R., N.A-H., Y.M., and C.W. approved final version of manuscript.

REFERENCES

1. **Hess EH**, **Polt JM.** Pupil size in relation to mental activity during simple problem-solving. *Science* 143: 1190–1192, 1964. doi:10.1126/science.143.3611.1190.
2. **Rajkowski J**, **Kubiak P**, **Aston-Jones G.** Locus coeruleus activity in monkey: phasic and tonic changes are associated with altered vigilance. *Brain Res Bull* 35: 607–616, 1994. doi:10.1016/0361-9230(94)90175-9.
3. **Joshi S**, **Gold JI.** Pupil size as a window on neural substrates of cognition. *Trends Cogn Sci* 24: 466–480, 2020. doi:10.1016/j.tics.2020.03.005.
4. **McDougal DH**, **Gamlin PD.** Autonomic control of the eye. *Compr Physiol* 5: 439–473, 2015. doi:10.1002/cphy.c140014.
5. **Coutinho JD**, **Huang J**, **Lefèvre P**, **Blohm G**, **Munoz DP.** Main sequence of human luminance-evoked pupil dynamics. *J Cogn Neurosci* 37: 840–852, 2025. doi:10.1162/jocn_a_02296.
6. **Bremner F.** Pupil evaluation as a test for autonomic disorders. *Clin Auton Res* 19: 88–101, 2009. doi:10.1007/s10286-009-0515-2.
7. **Szabadi E.** Functional organization of the sympathetic pathways controlling the pupil: light-inhibited and light-stimulated pathways. *Front Neurol* 9: 1069, 2018. doi:10.3389/fneur.2018.01069.
8. **El Haj M**, **Chapelet G**, **Moustafa AA**, **Boutoleau-Bretonnière C.** Pupil size as an indicator of cognitive activity in mild Alzheimer's disease. *EXCLI J* 21: 307–316, 2022. doi:10.17179/excli2021-4568.
9. **Strauch C**, **Wang C-A**, **Einhäuser W**, **Van der Stigchel S**, **Naber M.** Pupillometry as an integrated readout of distinct attentional networks. *Trends Neurosci* 45: 635–647, 2022. doi:10.1016/j.tins.2022.05.003.
10. **Thompson HS**, **Franceschetti AT**, **Thompson PM.** Hippus. Semantic and historic considerations of the word. *Am J Ophthalmol* 71: 1116–1120, 1971.
11. **Centeno M**, **Feldmann M**, **Harrison NA**, **Rugg-Gunn FJ**, **Chaudhary U**, **Falcon C**, **Lemieux L**, **Thom M**, **Smith SJM**, **Sisodiya SM.** Epilepsy causing pupillary hippus: an unusual semiology: Ictal Hippus. *Epilepsia* 52: e93–e96, 2011. doi:10.1111/j.1528-1167.2011.03137.x.
12. **Fernández-Torre JL**, **Paramio-Paz A**, **Lorda-de los Ríos I**, **Martín-García M**, **Hernández-Hernández MA.** Pupillary hippus as clinical manifestation of refractory autonomic nonconvulsive status epilepticus: pathophysiological implications. *Seizure* 63: 102–104, 2018. doi:10.1016/j.seizure.2018.11.006.
13. **Yoss RE**, **Moyer NJ**, **Hollenhorst RW.** Hippus and other spontaneous rhythmic pupillary waves. *Am J Ophthalmol* 70: 935–941, 1970. doi:10.1016/0002-9394 (70)92470-0.
14. **Bufo MR**, **Guidotti M**, **De Faria C**, **Mofid Y**, **Bonnet-Brilhault F**, **Wardak C**, **Aguillon-Hernandez N.** Autonomic tone in children and adults: pupillary, electrodermal and cardiac activity at rest. *Int J Psychophysiol* 180: 68–78, 2022. doi:10.1016/j.ijpsycho.2022.07.009.
15. **Schneider M**, **Hathway P**, **Leuchs L**, **Sämann PG**, **Czisch M**, **Spoormaker VI.** Spontaneous pupil dilations during the resting state are associated with activation of the salience network. *Neuroimage* 139: 189–201, 2016. doi:10.1016/j.neuroimage.2016.06.011.

16. **Parnandi A**, **Gutierrez-Osuna R.** Contactless measurement of heart rate variability from pupillary fluctuations. In: *2013 Humaine Association Conference on Affective Computing and Intelligent Interaction (ACII)*. IEEE, p. 191–196.
17. **Schaefer M**, **Mathôt S**, **Lundqvist M**, **Lundström JN**, **Arshamian A.** The pupillary respiratory-phase response: pupil size is smallest around inhalation onset and largest during exhalation. *J Physiol* 603: 1607–1625, 2025. doi:10.1113/JP287205.
18. **Turnbull PRK**, **Irani N**, **Lim N**, **Phillips JR.** Origins of pupillary hippus in the autonomic nervous system. *Invest Ophthalmol Vis Sci* 58: 197–203, 2017. doi:10.1167/iovs.16-20785.
19. **Burtis DB**, **Heilman KM**, **Mo J**, **Wang C**, **Lewis GF**, **Davilla MI**, **Ding M**, **Porges SW**, **Williamson JB.** The effects of constrained left versus right monocular viewing on the autonomic nervous system. *Biol Psychol* 100: 79–85, 2014. doi:10.1016/j.biopsycho.2014.05.006.
20. **Nakamura NH**, **Fukunaga M**, **Oku Y.** Respiratory fluctuations in pupil diameter are not maintained during cognitive tasks. *Respir Physiol Neurobiol* 265: 68–75, 2019. doi:10.1016/j.resp.2018.07.005.
21. **Schaefer M**, **Edwards S**, **Nordén F**, **Lundström JN**, **Arshamian A.** Inconclusive evidence that breathing shapes pupil dynamics in humans: a systematic review. *Pflugers Arch* 475: 119–137, 2023. doi:10.1007/s00424-022-02729-0.
22. **Bouma H**, **Baghuis LCJ.** Hippus of the pupil: periods of slow oscillations of unknown origin. *Vision Res* 11: 1345–1351, 1971. doi:10.1016/0042-6989 (71)90016-2.
23. **Calcagnini G**, **Censi F**, **Lino S**, **Cerutti S.** Spontaneous fluctuations of human pupil reflect central autonomic rhythms. *Methods Inf Med* 39: 142–145, 2000. doi:10.1055/s-0038-1634277.
24. **Kardon R.** Pupillary light reflex. *Curr Opin Ophthalmol* 6: 20–26, 1995. doi:10.1097/00055735-199512000-00004.
25. **Bouma H.** Size of the static pupil as a function of wave-length and luminosity of the light incident on the human eye. *Nature* 193: 690–691, 1962. doi:10.1038/193690a0.
26. **Beatty J.** Task-evoked pupillary responses, processing load, and the structure of processing resources. *Psychol Bull* 91: 276–292, 1982.
27. **Murata A**, **Iwase H.** Evaluation of mental workload by variability of pupil area. *IEICE Trans Inf Syst* E83-D: 1187–1190, 2000.
28. **Reimer J**, **Froudarakis E**, **Cadwell CR**, **Yatsenko D**, **Denfield GH**, **Tolias AS.** Pupil fluctuations track fast switching of cortical states during quiet wakefulness. *Neuron* 84: 355–362, 2014. doi:10.1016/j.neuron.2014.09.033.
29. **Robison MK**, **Coyne JT**, **Sibley C**, **Brown NL**, **Neilson B**, **Foroughi C.** An examination of relations between baseline pupil measures and cognitive abilities. *Psychophysiology* 59: e14124, 2022. doi:10.1111/psyp.14124.
30. **Mathur A**, **Gehrmann J**, **Atchison DA.** Influences of luminance and accommodation stimuli on pupil size and pupil center location. *Invest Ophthalmol Vis Sci* 55: 2166–2172, 2014. doi:10.1167/iovs.13-13492.
31. **Stockman A**, **Sharpe LT.** Into the twilight zone: the complexities of mesopic vision and luminous efficiency. *Ophthalmic Physiol Opt* 26: 225–239, 2006. doi:10.1111/j.1475-1313.2006.00325.x.
32. R: The R Project for Statistical Computing [Online]. https://www.r-project.org/ [2025 Sept 11].
33. **Bolar K.** STAT: Interactive Document for Working with Basic Statistical Analysis [Online]. https://cran.r-project.org/web/packages/STAT/index.html [2025 Sept 11].
34. **Fox J**, **Weisberg S**, **Price B**, **Adler D**, **Bates D**, **Baud-Bovy G**, **Bolker B**, **Ellison S**, **Firth D**, **Friendly M**, **Gorjanc G**, **Graves S**, **Heiberger R**, **Krivitsky P**, **Laboissiere R**, **Maechler M**, **Monette G**, **Murdoch D**, **Nilsson H**, **Ogle D**, **Ripley B**, **Short T**, **Venables W**, **Walker S**, **Winsemius D**, **Zeileis A**, **R-Core.** car: Companion to Applied Regression [Online]. https://cran.r-project.org/web/packages/car/index.html [2025 Sept 11].
35. **Bates D**, **Mächler M**, **Bolker B**, **Walker S.** Fitting linear mixed-effects models using lme4. *J Stat Soft* 67: 1–48, 2015. doi:10.18637/jss.v067.i01.
36. **Maechler M, Rousseeuw P, Struyf A, Hubert M, Hornik K.** cluster: Cluster Analysis Basics and Extensions. https://cran.r-project.org/package=cluster [2025 Sept 11].
37. **Wickham H.** Data analysis. In: *ggplot2: Elegant Graphics for Data Analysis*. Springer International Publishing, p. 189–201.
38. **Wei T**, **Simko V**, **Levy M**, **Xie Y**, **Jin Y**, **Zemla J**, **Freidank M**, **Cai J**, **Protivinsky T.** corrplot: Visualization of a Correlation Matrix [Online]. https://cran.r-project.org/web/packages/corrplot/index.html [11 Sept 2025].
39. **Scalia F**, **Arango V.** Topographic organization of the projections of the retina to the pretectal region in the rat. *J Comp Neurol* 186: 271–292, 1979. doi:10.1002/cne.901860210.
40. **Warga M**, **Lüdtke H**, **Wilhelm H**, **Wilhelm B.** How do spontaneous pupillary oscillations in light relate to light intensity? *Vision Res* 49: 295–300, 2009. doi:10.1016/j.visres.2008.09.019.
41. **Loewenfeld IE.** *The Pupil: Anatomy, Physiology, and Clinical Applications*. Butterworth-Heinemann, 1999.
42. **Joshi S**, **Li Y**, **Kalwani RM**, **Gold JI.** Relationships between pupil diameter and neuronal activity in the locus coeruleus, colliculi, and cingulate cortex. *Neuron* 89: 221–234, 2016. doi:10.1016/j.neuron.2015.11.028.
43. **Noudoost B**, **Chang MH**, **Steinmetz NA**, **Moore T.** Top-down control of visual attention. *Curr Opin Neurobiol* 20: 183–190, 2010. doi:10.1016/j.conb.2010.02.003.
44. **Binda P**, **Murray SO.** Keeping a large-pupilled eye on high-level visual processing. *Trends Cogn Sci* 19: 1–3, 2015. doi:10.1016/j.tics.2014.11.002.
45. **Wang C-A**, **Brien DC**, **Munoz DP.** Pupil size reveals preparatory processes in the generation of pro-saccades and anti-saccades. *Eur J Neurosci* 41: 1102–1110, 2015. doi:10.1111/ejn.12883.
46. **Wang C-A**, **Boehnke SE**, **White BJ**, **Munoz DP.** Microstimulation of the monkey superior colliculus induces pupil dilation without evoking saccades. *J Neurosci* 32: 3629–3636, 2012. doi:10.1523/JNEUROSCI.5512-11.2012.
47. **Aston-Jones G**, **Cohen JD.** An integrative theory of locus coeruleus-norepinephrine function: adaptive gain and optimal performance. *Annu Rev Neurosci* 28: 403–450, 2005. doi:10.1146/annurev.neuro.28.061604.135709.
48. **Gilzenrat MS**, **Nieuwenhuis S**, **Jepma M**, **Cohen JD.** Pupil diameter tracks changes in control state predicted by the adaptive gain theory of locus coeruleus function. *Cogn Affect Behav Neurosci* 10: 252–269, 2010. doi:10.3758/CABN.10.2.252.
49. **Murphy PR**, **Robertson IH**, **Balsters JH**, **O'connell RG.** Pupillometry and P3 index the locus coeruleus-noradrenergic arousal function in humans. *Psychophysiology* 48: 1532–1543, 2011. doi:10.1111/j.1469-8986.2011.01226.x.
50. **Mathôt S**, **van der Linden L**, **Grainger J**, **Vitu F.** The pupillary light response reveals the focus of covert visual attention. *PLoS One* 8: e78168, 2013. doi:10.1371/journal.pone.0078168.
51. **Steinhauer SR**, **Condray R**, **Kasparek A.** Cognitive modulation of midbrain function: task-induced reduction of the pupillary light reflex. *Int J Psychophysiol* 39: 21–30, 2000. doi:10.1016/s0167-8760(00)00119-7.
52. **van der Wel P**, **van Steenbergen H.** Pupil dilation as an index of effort in cognitive control tasks: a review. *Psychon Bull Rev* 25: 2005–2015, 2018. doi:10.3758/s13423-018-1432-y.
53. **Hafed ZM**, **Krauzlis RJ.** Goal representations dominate superior colliculus activity during extrafoveal tracking. *J Neurosci* 28: 9426–9439, 2008. doi:10.1523/JNEUROSCI.1313-08.2008.
54. **Beatty J**, **Lucero-Wagoner B.** The pupillary system. In: *Handbook of psychophysiology* (2nd edn.). Cambridge University Press, 2000, p. 142–162.
55. **Reimer J**, **McGinley MJ**, **Liu Y**, **Rodenkirch C**, **Wang Q**, **McCormick DA**, **Tolias AS.** Pupil fluctuations track rapid changes in adrenergic and cholinergic activity in cortex. *Nat Commun* 7: 13289, 2016. doi:10.1038/ncomms13289.
56. **Krejtz K**, **Duchowski AT**, **Niedzielska A**, **Biele C**, **Krejtz I.** Eye tracking cognitive load using pupil diameter and microsaccades with fixed gaze. *PLoS One* 13: e0203629, 2018. doi:10.1371/journal.pone.0203629.
57. **Annerer-Walcher S**, **Ceh SM**, **Putze F**, **Kampen M**, **Körner C**, **Benedek M.** How reliably do eye parameters indicate internal versus external attentional focus? *Cogn Sci* 45: e12977, 2021. doi:10.1111/cogs.12977.
58. **Benedek M**, **Stoiser R**, **Walcher S**, **Körner C.** Eye behavior associated with internally versus externally directed cognition. *Front Psychol* 8: 1092, 2017. doi:10.3389/fpsyg.2017.01092.

59. **Krauzlis RJ**, **Goffart L**, **Hafed ZM.** Neuronal control of fixation and fixational eye movements. *Philos Trans R Soc Lond B Biol Sci* 372: 20160205, 2017. doi:10.1098/rstb.2016.0205.
60. **Bouret S**, **Sara SJ.** Network reset: a simplified overarching theory of locus coeruleus noradrenaline function. *Trends Neurosci* 28: 574–582, 2005. doi:10.1016/j.tins.2005.09.002.
61. **Ebitz RB**, **Platt ML.** Neuronal activity in primate dorsal anterior cingulate cortex signals task conflict and predicts adjustments in pupil-linked arousal. *Neuron* 85: 628–640, 2015. doi:10.1016/j.neuron.2014.12.053.
62. **Unsworth N**, **Robison MK.** Tracking arousal state and mind wandering with pupillometry. *Cogn Affect Behav Neurosci* 18: 638–664, 2018. doi:10.3758/s13415-018-0594-4.
63. **Mathewson KE**, **Lleras A**, **Beck DM**, **Fabiani M**, **Ro T**, **Gratton G.** Pulsed out of awareness: EEG alpha oscillations represent a pulsed-inhibition of ongoing cortical processing. *Front Psychol* 2: 99, 2011. doi:10.3389/fpsyg.2011.00099.
64. **de Gee JW**, **Knapen T**, **Donner TH.** Decision-related pupil dilation reflects upcoming choice and individual bias. *Proc Natl Acad Sci USA* 111: E618–625, 2014. doi:10.1073/pnas.1317557111.
65. **Kahneman D**, **Beatty J.** Pupil diameter and load on memory. *Science* 154: 1583–1585, 1966. doi:10.1126/science.154.3756.1583.
66. **Yellin D**, **Berkovich-Ohana A**, **Malach R.** Coupling between pupil fluctuations and resting-state fMRI uncovers a slow build-up of antagonistic responses in the human cortex. *Neuroimage* 106: 414–427, 2015. doi:10.1016/j.neuroimage.2014.11.034.